

Molecular Docking Investigation and Pharmacokinetic Properties Prediction of Some Benzimidazole Analogues as Dihydropteroate Synthase (DHPS) Inhibitors

Christiana Abimbola Salubi (✉ 3878010@myuwc.ac.za)

University of the Western Cape

Article

Keywords: ADMET, Sulfamethoxazole, Sulfamethazine, benzimidazole, Antimicrobial

Posted Date: July 28th, 2023

DOI: <https://doi.org/10.21203/rs.3.rs-3167170/v1>

License:  This work is licensed under a Creative Commons Attribution 4.0 International License. [Read Full License](#)

Abstract

Recent research has established the classification of benzimidazole as a privileged structure owing to its strong binding affinity to protein receptors and diverse enzymes. Extensive investigations have consistently shown the antimicrobial potential of benzimidazole derivatives against a wide range of microbial strains. In order to gain a deeper understanding of the relationship between structural modifications and the antibacterial effectiveness of sulfonamide compounds, we have developed targeted derivatives with subtle alterations in the aromatic ring of sulfonamides and the substituent groups. Furthermore, we present the results of molecular docking analyses, ADMET properties, and drug-likeness assessment to evaluate the potential of these compounds to interact with dihydropteroate synthase, a key enzyme involved in bacterial growth. The compounds exhibited a favourable binding affinity, ranging from 7.1 to 7.9 kcal/mol, which surpasses that of the standard drugs sulfamethazine and sulfamethoxazole, with binding affinities of 5.9 and 6.1 kcal/mol, respectively. Furthermore, these compounds demonstrated good oral bioavailability and exhibited favourable drug-like properties.

1. Introduction

In several countries, especially those that are developing, microbial infections and their treatments pose significant challenges. The emergence of drug resistance is a major contributing factor, leading to a staggering annual global death toll exceeding 700,000. The use of commonly prescribed antimicrobial drugs such as ciprofloxacin, amoxicillin, and norfloxacin has resulted in various complications, including adverse side effects and the development of resistance, further exacerbating the problem.^{1,2} Microorganisms have evolved at a faster pace than the discovery of new effective compounds, and the widespread misuse of antibacterial compounds has contributed to a troubling surge in microbial resistance. The pursuit of new candidates for antibacterial drugs employs various strategies, including: i) systematic screening of synthetic library compounds; ii) structural modification of known drugs; iii); exploration of natural products guided by ethnopharmacology and iv) *in silico* design of novel molecules. Within this scope, numerous compounds based on sulfonamides have been utilized to create potent lead substances with improved efficacy and reduced toxicity.³ Antibiotic resistance poses a daunting challenge in the field of public health, leading to a substantial burden caused by infections from multidrug-resistant (MDR) microorganisms on a global scale. The declining efficacy of antibiotics presents a pressing issue within the public health system, necessitating the development of novel drug candidates or modification of existing antibiotics to combat resistance.

Over the past few decades, the prevalence of multidrug-resistant pathogenic bacteria has become increasingly common, prompting the exploration of modifying obsolete antibiotics or control agents to effectively manage MDR bacteria.⁴ In 1935, Gerhard Domagk discovered the antimicrobial characteristics of the azo dye Prontosil (Fig. 1), which subsequently paved the way for the development of sulfa drugs. Over the years, a vast array of sulfonamide derivatives has been documented, showcasing diverse biological activities beyond their recognized antibacterial properties. Moreover, the sulfonamide group has been incorporated into established biologically significant frameworks to yield novel effects.⁵ Sulfonamide drugs have been shown to possess broad antibacterial activity by inhibiting the dihydropteroate synthase (DHPS) enzyme.⁶ Herein, sulfonamides hinder bacterial growth by specifically targeting the enzyme dihydropteroate synthase (DHPS) within the folate pathway. DHPS facilitates the condensation of 6-hydroxymethyl-7,8-dihydropterin-pyrophosphate (DHPPP) and p-aminobenzoic acid (PABA) to form dihydropteroate (DHpt). The mechanism of action of antimicrobial sulfonamides involves their role as competitive inhibitors of PABA, thereby impeding the biosynthesis of dihydrofolic acid. Consequently, the growth and reproduction of microorganisms are hindered.⁷

Over the years, benzimidazole has garnered significant interest since the 1800s, and it is found in numerous natural compounds as well as in various drugs such as dovitinib, galeterone, rabeprazole, omeprazole, albendazole, etonitazine, lansoprazole, tenatoprazole, and mavatrep.⁸ In 1872, Hoebrecker accomplished the first synthesis of benzimidazole, specifically 2, 5 (or 2, 6)-dimethylbenzimidazole, from 2-nitro-4-methylacetanilide.⁹ The benzimidazole structure consists of a fused imidazole ring with a benzene ring, making it a crucial heterocyclic pharmacophore. Benzimidazole moieties are present in a wide range of clinically useful drugs, which exhibit diverse biological activities and possess intriguing chemistry.¹⁰ In 1943, Goodman and Nancy Hart were the first to publish a research article on the pharmacological properties of benzimidazole, followed by Woodley reporting its antibacterial activity in 1944. Previous research has underscored the significance of benzimidazole in heterocyclic systems.¹¹ Studies have revealed that benzimidazole is classified as a privileged structure due to its affinity for protein receptors and various enzymes¹². Numerous studies have demonstrated the antimicrobial activity of benzimidazole derivatives against a variety of microorganism strains.¹³ The most straightforward pathway for synthesizing 1H-benzimidazole involves condensing carboxylic acid (or its derivatives such as orthoesters, nitriles, and chlorides) with o-phenylenediamine in the presence of an aldehyde or acid, utilizing sodium (Na₂S₂O₅).¹⁴ The biological activity of benzimidazole stems from its distinctive physicochemical properties, including π→π stacking interactions, hydrophobic interactions, coordination as a ligand with metals, H-bond acceptor/donor capability, and its ability to bind with nucleic acids, enzymes, and biomolecules. These properties contribute to the diverse range of biological effects exhibited by benzimidazole compounds.¹⁵ Structural modifications of benzimidazole are necessary to enhance stability, bioavailability, and biological profiles. Consequently, benzimidazole has attracted significant attention as an antimicrobial,¹⁶ antidiabetic,¹⁷ antioxidant,¹¹ anticancer,¹⁸ antiprotozoal, anticonvulsant and diuretics agent owing to the ability to alter substituents around its core structure. However, it should be noted that introducing a substituent at the para-position of the aniline moiety of benzimidazole derivatives leads to a reduction in antibacterial activity.¹⁹

In the research conducted on pyrazoles-sulfonamide hybrid (PSH) compounds, it was observed that pyrazole derivatives containing a sulfonamide group exhibited significant antimicrobial activity compared to pyrazole when evaluated as antimicrobial agents.²⁰ Molecular docking analysis was conducted against the dihydropteroate synthase (DHPS) receptors of *Staphylococcus aureus* and *Escherichia coli* bacterial strains. The findings revealed that the sulfonamide complexes fit well within the active sites of the receptors and were stabilized by hydrogen bonds and hydrophobic interactions. This suggests their potential as inhibitors, which aligns with the observed strong antimicrobial activity of the compounds.²¹ The computational analysis, including molecular docking and molecular dynamics simulations, yielded compelling results regarding the N-acylsulphonamide derivatives. These derivatives demonstrated a high docking score, excellent stability, and favourable intermolecular interactions within the binding pocket of dihydropteroate synthases (DHPS) when compared to the reference ligand, sulfamethoxazole. Furthermore, the acylsulfonamide compounds were evaluated for in vitro antimicrobial activity against 13 microbial strains using the well diffusion method. Remarkably, the results exhibited notable activity against the tested microorganisms, with inhibition diameters ranging from 16mm to 34mm. Importantly, no apparent distinction in activity was observed between Gram-positive and Gram-negative bacteria.²²

Sulfonyl derivatives derived from amino acids and benzenesulfonyl chloride have exhibited potent antibacterial activity, surpassing that of conventional drugs such as penicillin.²³ Furthermore, the synthesized compounds exhibited compelling and enhanced antimicrobial activity in comparison to the reference drugs, with minimum inhibitory concentration (MIC) values ranging from 3.9 to 31.3 µg/mL against a range of Gram-positive and Gram-negative bacteria.²⁴ The presence of certain functional groups, such as (C = O and O = C-NH₂), is believed to contribute to this activity by potentially augmenting the hydrophobic characteristics, liposolubility, and biological absorbance of the

molecules.²⁵ The utilization of trimethoprim–sulfamethoxazole (TMP-SMX) has been linked to severe and potentially life-threatening adverse drug reactions that are presumed to be immune-mediated idiosyncratic in nature. These drug adverse reactions include toxic epidermal necrolysis (TEN), severe drug-induced liver injury (DILI), Stevens-Johnson syndrome (SJS), blood dyscrasia and drug reactions with eosinophilia and systemic symptoms. It is noteworthy that TMP-SMX ranks among the top five causes of DILI in the United States. The specific risk factors contributing to liver injury associated with TMP-SMX remain largely unidentified, it is common among African Americans and individuals infected with the human immunodeficiency virus (HIV).²⁶

To enhance our comprehension of how structural modification impact the antibacterial efficacy of sulfonamide compounds, we design specific derivatives with subtle modifications on the aromatic ring of sulfonamides, and in the nature of the substituent group. Additionally, we provide molecular docking outcomes, ADMET properties, and drug-likeness that assess the ability of these compounds to interact with dihydropteroate synthase, a crucial enzyme for bacterial proliferation. This analysis directly indicates the antibacterial properties of the compounds under investigation. This research study will be valuable to researchers who specifically work in the medicinal chemistry field to visualize the pharmacological activities of new benzimidazole derivatives by developing a structure-activity relationship of benzimidazole drugs.

2. Materials and Methods

2.1 Proteins and Ligands Accession

The crystal structure of DPHS enzymes complexed with an OH-CH₂-Pterin-Pyrophosphate inhibitor, used for evaluation in this study, was obtained from the RCSB Protein Data Bank (PDB ID: 1AD4). The structures were retrieved in PDB format.^{27,28} A library of compounds comprising 12 benzimidazole sulfone ligands (Fig. 1) was designed using MarvinSketch and then saved in the sdf format. These compounds were intended to be explored as novel antimicrobial agents targeting the dihydropteroate synthase (DHPS) enzyme, known for its role as a DHPS inhibitor.

2.2 Protein preparation

To assess their inhibitory potential, benzimidazole derivatives were subjected to docking studies with DPHS protein. The docking analysis included benzimidazole derivatives as well as standard drugs, sulfamethazine and sulfamethoxazole, targeting DPHS inhibitors. The Autodock Vina virtual screening tool and Discovery Studio (DS) were utilized for conducting the docking study.²⁹ Prior to docking, protein preparation was done using the "UCSF Chimera Tool" to eliminate water molecules and native ligands.

2.3 Target and ligand optimization

The XYZ coordinates of the binding site sphere for protein 1AD4 were determined as 59.0503, 57.6767, and 25.0000. These coordinates exhibited a stable conformation and minimal energy. The optimization of the target protein and benzimidazole derivative was performed using the UCSF Chimera tool and Drug Discovery Studio. The interactions of the docked poses were further analyzed using the Discovery Studio (DS) Visualizer. The entire docking experiment was executed on a processor with specifications: Intel(R) Core(TM) i5-8250U CPU @ 1.60GHz 1.80 GHz, 64-bit architecture. Sulfamethazine and sulfamethoxazole were retrieved from Pubchem database.

3. Results and Discussion

Computer-Aided Drug Design (CADD) presents a valuable alternative to the resource-intensive and time-consuming process of drug design and development. In this study, benzimidazole derivatives were subjected to docking studies

with DHPS, alongside the standard drugs. The docking results are summarized in Table 1. The selection of these derivatives for docking studies was based on the known medicinal benefits exhibited by sulfa and benzimidazole compounds. This prompted us to investigate the interaction of both compound classes with DHPS as potential antimicrobial agents.³⁰ The favourable minimum binding energies obtained indicate the successful docking of benzimidazole inhibitors and the standard drug to the DHPS protein (Table 1). Furthermore, the potential binding sites of benzimidazole within the DHPS active sites were identified as Asn11, Arg52, Asp84, Asn103, Asp167, and Lys203 for 1AD4. Notably, benzimidazole derivatives demonstrated superior binding affinity compared to sulfamethoxazole and sulfamethazine, the standard drugs employed.

Table 1
Binding energy (kcal/mol)

Compounds	Binding affinities kcal/mol	Protein (Binding site)
1a	7.1	Lys207 (2.47 Å) Conventional H-bond, Ser201 (3.56 Å) Lys203 (3.57 Å) C-H bond Asp213 (3.91 Å) π Anion Arg219 (3.61 Å) π cation
1b	7.4	Arg204 (1.89 Å), Arg202 (2.00 Å) Conventional H-bond, Pro53 (4.89 Å) Arg52 (4.07 Å, 4.50 Å) Alky bond Arg204 (3.87 Å), Phe172 (5.03 Å) π Alkyl Phe172 (5.04 Å) π alkyl Arg52 (3.70 Å) π cation
1c	7.2	Ser50 (3.29 Å), Asn11 (3.52 Å) C-H bond Gln105 (1.45 Å), Arg204 (2.03 Å) unfavourable donor -donor Arg52 (4.14 Å) Alky Arg204 (5.20 Å) π-alkyl Arg52 (3.97 Å, 3.56 Å) π cation
1d	7.9	Gln105 (2.43 Å) Conventional H-bond, Lys203 (3.51 Å) C-H bond
1e	7.2	Arg202 (2.51 Å), Arg52 (2.22 Å), Arg219 (2.30 Å) Conventional H-bond, Ala173 (3.86 Å) Pro53 (4.04 Å), Arg202 (4.15 Å), Pro216 (4.79 Å) Alky bond His241 (4.29 Å), Pro216 (5.10 Å), Arg204 (4.96 Å) π-alkyl Arg219 (4.30 Å) π cation
1f	7.1	Arg204 (2.35 Å), Arg239 (2.33 Å) Conventional H-bond, Lys203 (3.38 Å), His241(3.22 Å) C-H bond Phe172 (5.04 Å) Lys203 (4.17 Å) π-Alkyl His241 (5.09 Å) π -sulfur
2a	7.3	Arg52 (2.61, 2.72 Å), Lys174 (2.68 Å) Conventional H-bond. Gly133 (3.69 Å) C-H bond Arg204 (4.19 Å), Lys203 (4.35 Å), His241 (4.40 Å) π-alkyl Arg219 (5.10 Å), Arg52 (4.33 Å) unfavourable Positive-positive Arg204 (2.23 Å) unfavourable donor-donor Arg52 (3.28 Å), Arg204 (4.61 Å) π cation

Compounds	Binding affinities kcal/mol	Protein (Binding site)
2b	7.6	Asp42 (2.48 Å), Gly40 (3.03 Å) Conventional H-bond, Lys248 (4.03 Å), Lys251 (4.99 Å) Alky bond Lys251 (4.96 Å) π cation Asp78 (5.16 Å) Attractive charge Asp100 (4.00 Å), Asp78 (4.97 Å) π anion Ala247 (4.48 Å), 5.25 Å), Lys80 (4.44 Å) Π-alkyl
2c	7.5	Lys3 (2.71 Å), Gly98 (1.96 Å) Phe77 (2.53 Å) Asp42 (2.67 Å) Conventional H-bond, Asp42 (4.57 Å) Attractive charge Lys251 (4.18 Å) Ala247 (4.13 Å) Alky Lys80 (5.45 Å) π- Alkyl Lys80 (2.37 Å) unfavourable donor –donor Asp42 (3.76 Å) π anion Val79 (4.32 Å) Amide π- stacked
2d	7.8	Gln105 (2.47 Å) Lys207 (2.27 Å) Conventional H-bond, Asp213 (4.20 Å) Attractive charge
2e	7.3	Lys207 (2.43 Å) Conventional H-bond, Thr215 (3.61 Å) Lys203 (3.28 Å) C-H bond Met128 (5.02 Å) Alky Phe172 (4.98 Å) π -alkyl Phe172 (5.01 Å) π-π T-shaped Arg219 (4.71 Å) unfavourable Positive-positive Arg52 (3.85 Å) π cation Asp213 (3.88 Å) Attractive charge Arg219 (3.35 Å) π Donor H-bond
2f	7.1	Lys207 (2.54 Å) Conventional H-bond, Lys203 (3.67 Å), Thr215 (3.51 Å) C-H bond Phe172 (5.07 Å) π-π T-shaped Arg219 (4.49 Å) unfavourable Positive-positive Arg219 (3.31 Å) Arg52 (4.18 Å) π cation; π -donor hydrogen bond Asp213 (4.04 Å) Attractive charge

Compounds	Binding affinities kcal/mol	Protein (Binding site)
Sulfamethaxazole	6.1	Lys203 (2.85 Å), Arg202 (1.93 Å) Conventional H-bond, Lys203 (3.45 Å) C-H bond Phe172 (5.16 Å) Lys 203 (5.18) π Alky Phe172 (4.93 Å) π-π T-shaped Arg219 (2.59 Å) unfavourable donor-donor Arg52 (4.80 Å) Arg239 (5.25 Å) unfavourable positive-positive Arg239 (3.50 Å) π cation Met128 (4.70 Å) Alkyl
Sulfamethazine	5.9	Val49 (2.61 Å) Arg52 (2.49 Å) Conventional H-bond, Lys203 (3.74 Å) C-H bond Pro216 (4.09 Å), Arg202 (4.59 Å) Alky bond methyl His241 (5.29 Å) π-π T-shaped Arg52 (2.06 Å), Arg239 (5.57 Å) unfavourable Positive-positive Arg239 (4.33 Å) π cation

The docking results for all derivatives demonstrate significant inhibition of DHPS, ranging from compounds **1a** to **2f**. Notably, derivatives **1b**, **1d**, **2b**, and **2d** exhibit strong inhibition of DHPS, displaying binding affinities higher than the standard drugs and aligning with the reported experimental antimicrobial activity.^{31,32} These derivatives have the potential to serve as improved antimicrobial agents. In general, compounds **1a** to **1f** exhibit slight low binding affinity compared to **2a** to **2f**, which can be attributed to the structural differences in the sulfonamide derivatives. Specifically, derivatives **1b** and **1c** demonstrate stronger inhibition of DHPS when compared to sulfamethazine, which has a binding affinity of -5.9 kcal/mol. Furthermore, in comparison to the DHPS inhibitor sulfamethaxazole, derivative **2b** and **2d** exhibit robust inhibition of DHPS, surpassing the binding affinity of sulfamethaxazole (-6.1 kcal/mol).

3.1 Intermolecular Interaction

Compound **1a** formed a conventional hydrogen bond with Lys207 (2.47 Å) residue through the sulfonyl oxygen atom. Additionally, Ser201 (3.56 Å) and Lys203 (3.57 Å) form carbon-hydrogen bonds with the benzimidazole ring, effectively anchoring the ligands within the protein's binding pocket. The interaction of Asp213 (3.91 Å) and Arg219 (3.61 Å) residues involves electrostatic bond interactions (π Anion and π cation) with the π-orbital ring of sulfamethazine, as illustrated in Fig. 2.

Compound **1b** exhibits two conventional hydrogen bonds with Arg204 (1.89 Å) and Arg202 (2.00 Å) through sulfonyl oxygen and hydrogen atom of -NH. Several hydrophobic interactions are observed with Pro53 (4.89 Å: alkyl bond), Arg52 (4.07 Å, 4.50 Å: alkyl bond), Arg204 (3.87 Å: π alkyl), and Phe172 (5.03 Å and 5.04 Å: π alkyl). Notably, Arg52 (3.70 Å) prompts a hydrophobic interaction (π cation) at the protein's binding pocket with the sulfamethazine heteroaryl ring, as depicted in Fig. 3.

In the case of Compound **1c**, a carbon-hydrogen bond interaction is formed with Ser50 (3.29 Å) and Asn11 (3.52 Å) residues binding to DHPS active site, while an unfavorable donor-donor interaction occurs with Gln105 (1.45 Å) and Arg204 (2.03 Å). However, Arg52 (4.14 Å: alkyl bond) and Arg52 (3.97 Å, 3.56 Å: π cation) residues establish a hydrophobic interaction with the sulfamethazine aromatic ring at the protein's binding pocket. Furthermore, the hydrophobic bond interaction between Arg204 (5.20 Å: π-alkyl) residue and the ligand's π-orbital system is observed (Fig. 4).

Of particular significance, compound **1d**, which exhibited the highest binding affinity (-7.9 kcal/mol) among the benzimidazole derivatives, forms only two hydrogen bonds. These bonds are observed with Gln105 (2.43 Å: conventional hydrogen bond) and Lys203 (3.51 Å: carbon-hydrogen bond) residues, effectively binding the compound to the target's pocket, as shown in Fig. 5.

Compound **1e** demonstrates three interactions with the target protein. These interactions include hydrogen bonds with Arg202 (2.51 Å), Arg52 (2.22 Å), and Arg219 (2.30 Å) (conventional hydrogen bonds) through hydrogen atom of –NH, oxygen of carbonyl and sulfonyl oxygen atom respectively. Additionally, hydrophobic bonds are observed with Ala173 (3.86 Å), Pro53 (4.04 Å), Arg202 (4.15 Å), Pro216 (4.79 Å) (alkyl bonds), and His241 (4.29 Å), Pro216 (5.10 Å), Arg204 (4.96 Å) (π-alkyl). Finally, an electrostatic interaction is present with Arg219 (4.30 Å) (π cation), as depicted in Fig. 6.

Compound **1f** establishes two conventional hydrogen bonds, involving the oxygen atoms of both the carbonyl group (C = O) and the sulfonyl group (S = O), with Arg204 (2.35 Å) and Arg239 (2.33 Å) residues. Furthermore, two carbon-hydrogen bonds are formed with His241 (3.22 Å) and Lys203 (3.38 Å), effectively binding the compound to the target's pocket. Additionally, two hydrophobic bonds are observed with Phe172 (5.04 Å) and Lys203 (4.17 Å) (π-alkyl residues). Notably, a π-sulfur interaction occurs between His241 (5.09 Å) and the sulfonyl sulphur atom (Fig. 7). Ligand **1f** primarily interacts with the binding pocket of DHPS.

Compound **2a** establishes two conventional hydrogen bonds, one with Arg52 (2.61 Å) through the carbonyl oxygen (C = O) and another with Lys174 (2.68 Å) through the -NH hydrogen atom. A carbon-hydrogen interaction is formed with Gly133 (3.69 Å) residue, while hydrophobic interactions occur with Arg204 (4.19 Å), Lys203 (4.35 Å), and His241 (4.40 Å) (π-alkyl bonds) involving the π-orbital system of the sulfamethoxazole ring effectively binding to the target's pocket. Arg52 (3.28 Å) and Arg204 (4.61 Å) exhibit an electrostatic interaction (π cation) with the ligand's π-orbital ring. Additionally, the ligand interacts with Arg219 (5.10 Å), Arg52 (4.33 Å), and Arg204 (2.23 Å), leading to unfavorable positive-positive and unfavorable donor-donor interactions, respectively (Fig. 8).

Compound **2b**, which exhibits a favourable binding affinity of 7.6 kcal/mol, forms a conventional hydrogen bond with Asp42 (2.48 Å) and Gly40 (3.03 Å) through the -NH hydrogen and carbonyl oxygen (C = O), respectively. Hydrophobic bonds are observed with Lys248 (4.03 Å), Lys251 (4.99 Å) (alkyl bonds), Ala247 (4.48 Å, 5.25 Å) and Lys80 (4.44 Å) (π-alkyl bonds), involving the π-orbital ring of both sulfamethoxazole and the benzimidazole ring. Furthermore, an electrostatic interaction occurs with Lys251 (4.96 Å) (π cation), Asp100 (4.00 Å), and Asp78 (4.97 Å) (π anion) through the π-orbital system. Notably, the amino acid Asp78 (5.16 Å) forms an attractive charge interaction with the sulfonyl sulfur atom (Fig. 9).

Compound **2c** exhibits a conventional hydrogen bond with Lys3 (2.71 Å), Gly98 (1.96 Å), Phe77 (2.53 Å), and Asp42 (2.67 Å) through the sulfonyl oxygen, hydroxyl oxygen (OH), -NH hydrogen, and -NH hydrogen atom, respectively. Hydrophobic bonds are observed with Lys251 (4.18 Å), Ala247 (4.13 Å) (alkyl bond), Lys80 (5.45 Å) (π-alkyl bond), and Val179 (4.32 Å) (amide π-stacked bond), involving the methyl substituent and the pi-orbital ring of both the benzimidazole and sulfamethoxazole rings. Additionally, an electrostatic interaction occurs with Asp42 (3.76 Å) through the π-orbital system (π anion). Furthermore, Asp42 (4.57 Å) and Lys80 (2.37 Å) residues form an attractive

charge interaction and an unfavourable donor-donor interaction, respectively, through the sulfonyl sulfur and -NH hydrogen atom (Fig. 10).

Similar to compound **1d**, compound **2d** exhibits two conventional hydrogen bonds with Gln105 (2.47 Å) and Lys207 (2.27 Å) through the oxygen atoms of the NO₂ and the sulfonyl group, respectively. Additionally, Asp213 (4.20 Å) forms an attractive interaction with the sulfonyl sulfur atom (Fig. 11).

Compound **2e** forms a conventional hydrogen bond with Lys207 (2.43 Å) through the sulfonyl oxygen and a carbon-hydrogen bond with Thr215 (3.61 Å) and Lys203 (3.28 Å) through the π-orbital system of sulfamethaxazole and the nitrogen lone pair electron of the benzimidazole ring, respectively. Hydrophobic interactions are observed with Met128 (5.02 Å) (alkyl bond), Phe172 (4.98 Å) (π-alkyl bond), and Phe172 (5.01 Å) (π-π T-shaped bond). Arg219 residues exhibit an unfavorable positive-positive interaction (4.71 Å) and a π-donor hydrogen bond (3.35 Å) with the ligand's sulfonamide sulfur and the π-orbital aromatic ring of sulfamethoxazole, respectively. Additionally, an electrostatic interaction occurs with Arg52 (3.85 Å) (π-cation) binding to the target's pocket, and Asp213 (3.88 Å) forms an attractive charge interaction (Fig. 12).

Compound **2f** forms one conventional hydrogen bond with Lys207 (2.54 Å) through the sulfonyl oxygen (S = O) and two carbon-hydrogen bonds with Lys203 (3.67 Å) and Thr215 (3.51 Å). Additionally, hydrophobic interactions occur with Phe172 (5.07 Å) (π- π T-shaped) residue, facilitated by the π-orbital system of the benzimidazole. Arg219 (3.31 Å) and Arg52 (4.18 Å) exhibit both pi-cation and π-donor hydrogen interactions with the ligand. In conclusion, Arg219 (4.49 Å) forms an unfavorable positive-positive interaction, while Asp213 (4.04 Å) forms an attractive charge interaction with the ligand (Fig. 13).

Sulfamethoxazole exhibited a binding affinity of 6.1 kcal/mol and formed two conventional hydrogen bonds with Lys203 (2.85 Å) and Arg202 (1.93 Å) through the sulfonyl oxygen and the hydrogen atom of -NH, respectively. It also formed a carbon-hydrogen bond with Lys203 (3.45 Å) residue. Hydrophobic interactions were observed with Phe172 (5.16 Å), Lys203 (5.18 Å) (π-alkyl), Met128 (4.70 Å) (alkyl bond), and Phe172 (4.93 Å) (π-π T-shaped). Arg239 (3.50 Å) exhibited an electrostatic interaction (π-cation). However, Arg219 (2.59 Å) formed an unfavorable donor-donor interaction, while Arg52 (4.80 Å) and Arg239 (5.25 Å) exhibited unfavorable positive-positive interactions in the pocket of the target protein (Fig. 14).

Sulfamethazine exhibited a binding affinity of 5.9 kcal/mol and formed two conventional hydrogen bonds with Val49 (2.61 Å) and Arg52 (2.49 Å) through the hydrogen atom of -NH and the sulfonyl oxygen atom, respectively. A carbon-hydrogen bond was observed between Lys203 (3.74 Å) residue at the binding pocket of the target protein. Hydrophobic interactions were observed with Pro216 (4.09 Å), Arg202 (4.59 Å) (alkyl bond), and His241 (5.29 Å) (π-π T-shaped) residues, involving the methyl group and the π-orbital aromatic ring. Unfavorable positive-positive interactions were exhibited by Arg52 (2.06 Å) and Arg239 (5.57 Å) through the sulfonyl sulfur atom. Lastly, Arg239 (4.33 Å, π-cation) interacted through the π-orbital of the aromatic ring (Fig. 15)

3.2 Validation of docking

To validate the docking process, the ligand was removed from the protein and then redocked into the active site of the protein (1AD4). This step was performed to assess the efficiency of the docking procedure. The redocked complex was superimposed with the native co-crystallized pterin obtained from the Protein Data Bank (PDB), and the RMSD value was calculated using DS. The calculated RMSD value of 1.8850 Å shows the accuracy of the docking process because it falls with the acceptable range of ≤ 3.0 Å RMSD values (Fig. 16).³³ The pterin inhibitor exhibited precise binding to the active site, as evidenced by a favourable binding energy of -6.2 kcal/mol. Notably, several amino acid residues,

including Lys 203, Arg 52, Arg 239, Asn 11, Asp 84, Asp 167, His241, Val240, and Asn 103, were found to interact with the pterin moiety, further confirming the specific binding interactions.²⁷

3.3 Pharmacokinetic analysis (ADMET)

Poor pharmacokinetics has been identified as a major factor leading to the failure of many drugs in clinical trials. In this study, we investigated the pharmacokinetic properties of all compounds using the ADMET predictor (swissadme and Admetsar). The following pharmacokinetic parameters were analyzed: MlogP (lipophilicity), Pgp inhibition (p-glycoprotein substrate/inhibitor), log S (water solubility), BBB (blood-brain barrier permeability), hERG inhibition, hepatotoxicity, Caucasian colon adenocarcinoma cell (Caco-2 cells) permeability, CYP450 substrate and inhibitor (3A4 and 2D6), HIA (human intestinal absorption), acute oral toxicity, bioavailability score, and gastrointestinal effects.

Lipophilicity, which refers to the ability of a chemical compound to dissolve in lipids, oils, fats, and non-polar solvents, is a crucial physicochemical property that influences the transport of drugs across lipid structures and their interactions with target proteins. Additionally, the water solubility (log S) of the compounds was predicted, with a solubility threshold set at log S <-4. To assess lipophilicity and water solubility, the Lipinski's rule of five was applied, which states that a compound should have an MlogP value of no more than 5 to exhibit good lipophilicity (MlogP ≤ 5). Furthermore, the predicted BBB permeability for all derivatives was found to be low, indicating limited or no penetration into the brain and potentially reducing the risk of central nervous system damage. However, all values lie in the acceptable range as seen in Table 2.³⁴

The Human Intestinal Absorption (HIA) data represents a combined measure of drug bioavailability and absorption, indicating the ability of drugs to penetrate the intestinal barrier. A positive value is assigned to all compounds, which means HIA is above 30%, while a low gastrointestinal (GI) absorption was predicted.³⁵ Caco-2 permeability is commonly employed to assess the suitability of drugs for oral dosing and to investigate drug reflux. In our study, all compounds yielded negative values, indicating low intestinal absorption. The Bioavailability Score confirms that all compounds comply with the Lipinski's rule of five (ROF), which suggests favourable pharmacokinetic properties (Table 3). The predicted hepatotoxicity values showed positive results with 40–50% similarity and probability values ranging from 0.53 to 0.55, indicating a low likelihood of hepatotoxicity. It is worth noting that some sulphonamides are known to exhibit hepatotoxicity.³⁶ The human cytochrome P450 (CYP) enzymes, particularly the isoforms CYP2D6 and CYP3A4, play a crucial role in drug metabolism and clearance in the liver. Inhibition of these enzymes can lead to compromised drug metabolism and potential drug-drug interactions. However, our results demonstrated that all compounds (**1a** to **2f**) showed no inhibition or substrate activity towards CYP2D6 (Table 2) similar to sulfamethoxazole. This suggests that these compounds can be efficiently metabolized by CYP2D6 and cleared from the body, thereby reducing the likelihood of toxicity.

It is noteworthy that all compounds except **1a**, **1e**, and **2a** were identified as non-inhibitors of CYP3A4. However, all compounds **1a** to **2f** exhibited substrate activity for CYP3A4. This indicates a potential risk of drug metabolism failure and drug-drug interactions. The human toxicity assessment was performed using the hERG inhibition model, which identifies genes sensitive to drug binding and predicts the risk of cardiotoxicity. According to the ADMET properties, compounds **1a**, **1c**, and **1d** showed no inhibition of hERG³⁷. Moreover, it was observed that all compounds, except **2c**, **2d**, and **2f**, exhibited inhibition of p-glycoprotein, while all compounds, except **2a**, **2d**, and **2e**, acted as substrates for p-glycoprotein. It is important to note that being a non-inhibitor and non-substrate for these proteins implies that the drugs can be easily eliminated from cells and are less likely to interact with other drugs.³⁸

Table 2
Admet Properties of benzimidazole derivatives.

Properties	Compounds											
	1a	1b	1c	1d	1e	1f	2a	2b	2c	2d	2e	2f
^a MlogP	0.24	1.00	-0.39	-0.67	1.22	0.38	0.24	0.60	-0.39	-0.68	1.22	0.37
^b ESOL Log S	-2.98	-3.09	-2.76	-2.97	-3.38	-3.07	-2.66	-2.78	-2.45	-2.66	-3.07	-2.76
HIA	+	+	+	+	+	+	+	+	+	+	+	+
Acute Oral Toxicity (c)	III	III	III	III	III	III	III	III	III	III	III	III
Blood Brain Barrier	No	No	No	No	No	No	No	No	No	No	No	No
Hepatotoxicity	+	+	+	+	+	+	+	+	+	+	+	+
Caco-2	-	-	-	-	-	-	-	-	-	-	-	-
Pgp substrate	-	-	-	-	-	-	+	-	-	+	+	-
Pgp inhibitor	+	+	+	+	+	+	+	+	-	-	+	-
CYP2D6 inhibition	-	-	-	-	-	-	-	-	-	-	-	-
CYP2D6 substrate	-	-	-	-	-	-	-	-	-	-	-	-
CYP3A4 inhibition	+	-	-	-	+	-	+	-	-	-	-	-
CYP3A4 substrate	+	+	+	+	+	+	+	+	+	+	+	+
GI absorption	Low	Low	Low	Low	Low	Low	Low	Low	Low	Low	Low	Low
hERG	-	+	-	-	+	+	+	+	+	+	+	+
Synthetic accessibility	5.06	4.99	4.90	5.12	5.12	4.84	4.95	4.91	4.80	5.03	5.04	4.76

^aMlogP \leq 5; ^blog S scale: insoluble < -10 < poorly < -6 < moderately < -4 < soluble < -2 < very < 0 < highly; ^cFrom 1 (very easy) to 10 (very difficult)

The drug-likeness of the benzimidazole derivatives was predicted to assess their potential as antimicrobial agents. All compounds, except **1b**, **1e**, **1f**, **2b**, **2e**, and **2f**, violated one condition of Lipinski's rule of five (Table 3), specifically the requirements calculated are Log P value \leq 5, the number of H-bond donors \leq 5, molecular weight \leq 500, and the number of H-bond acceptors \leq 10. However, these violations still fall within the acceptable range for oral bioavailability of drug molecules. The compound achieved a bioavailability score of 0.55, indicating favourable drug-like properties.

Table 3
Drug-likeness of the compounds

Compounds	Molecular weight	No. of H-bond acceptor	No of H-bond donor	No of Lipinski violation	Drug-likeness	Bioavailability score
1a	483.54	9	4	1	Yes	0.55
1b	467.54	8	4	0	Yes	0.55
1c	469.52	9	5	1	Yes	0.55
1d	498.51	10	4	1	Yes	0.55
1e	481.57	8	4	0	Yes	0.55
1f	453.52	8	4	0	Yes	0.55
2a	458.49	9	4	1	Yes	0.55
2b	442.49	8	4	0	Yes	0.55
2c	444.46	9	5	1	Yes	0.55
2d	473.46	10	4	1	Yes	0.55
2e	456.52	8	4	0	Yes	0.55
2f	428.46	8	4	0	Yes	0.55

4. Conclusion

Pharmacokinetic studies and molecular docking were conducted on 12 benzimidazole derivatives as DHPS inhibitors. The findings confirmed the inhibitory effect of the reported compounds and assessed their safety through pharmacokinetic profiling, suggesting their potential as antimicrobial drugs. Molecular docking analysis of the 12 benzimidazole derivatives with DHPS proteins of *Staphylococcus aureus* revealed that four derivatives, namely, **1b**, **1d**, **2b**, and **2d**, demonstrated potential activity with good oral bioavailability and low toxicity based on ADMET data. Considering toxicity is crucial in the field of drug design and medicinal chemistry. The compounds under investigation are considered suitable for drug development since they adhere to all necessary toxicity and pharmacokinetic properties. These results provide valuable insights for chemists, encouraging further synthesis of substituted benzimidazole derivatives for future drug design.

Declarations

Data Availability

All datasets generated during and/or analysed during the current study are available from the corresponding author on reasonable request.

I hereby confirm that there is no conflict of interest related to the manuscript.

Acknowledgments

I am grateful to NRF for funding towards the Postdoctoral Fellowship

References

1. Arshad, M. & Matiychuk, V. Substituted Pyrimidine-Sulfonamide Derivatives: Computational, Synthesis, Characterization, Anti-bacterial, MTT and Molecular Docking Assessment. *Biointerface Research in Applied Chemistry* **13** (2022). <https://doi.org/10.33263/briac133.239>
2. Aziz, D. M. & Azeez, H. J. Synthesis of new β -lactam- N-(thiazol-2-yl)benzene sulfonamide hybrids: Their in vitro antimicrobial and in silico molecular docking studies. *J Mol Struct* **1222** (2020). <https://doi.org/10.1016/j.molstruc.2020.128904>
3. Azevedo-Barbosa, H. *et al.* Design, Synthesis, Antimicrobial Evaluation and in Silico Studies of Eugenol-Sulfonamide Hybrids. *Chem Biodivers* **18**, e2100066 (2021). <https://doi.org/10.1002/cbdv.202100066>
4. Kumar Bishoyi, A., Mahapatra, M., Sahoo, C. R., Kumar Paidesetty, S. & Nath Padhy, R. Design, molecular docking and antimicrobial assessment of newly synthesized p-cuminal-sulfonamide Schiff base derivatives. *J Mol Struct* **1250** (2022). <https://doi.org/10.1016/j.molstruc.2021.131824>
5. Apaydin, S. & Torok, M. Sulfonamide derivatives as multi-target agents for complex diseases. *Bioorg Med Chem Lett* **29**, 2042-2050 (2019). <https://doi.org/10.1016/j.bmcl.2019.06.041>
6. Azzam, R. A., Elboshi, H. A. & Elgemeie, G. H. Synthesis, Physicochemical Properties and Molecular Docking of New Benzothiazole Derivatives as Antimicrobial Agents Targeting DHPS Enzyme. *Antibiotics (Basel)* **11** (2022). <https://doi.org/10.3390/antibiotics11121799>
7. Naaz, F. *et al.* Molecular modeling, synthesis, antibacterial and cytotoxicity evaluation of sulfonamide derivatives of benzimidazole, indazole, benzothiazole and thiazole. *Bioorg Med Chem* **26**, 3414-3428 (2018). <https://doi.org/10.1016/j.bmc.2018.05.015>
8. Küçükbay, H., Uçkun, M., Apohan, E. & Yeşilada, Ö. Cytotoxic and antimicrobial potential of benzimidazole derivatives. *Arch. Pharm.* **354**, 1-8 (2021). <https://doi.org/10.1002/ardp.202100076>
9. Gajanan, G. *et al.* A Review on Benzimidazole and it's Biological Activities. *Journal of Pharmaceutical Chemistry and Drug Formulation* **3**, 23-32 (2021).
10. Hashem, H. E. & El Bakri, Y. An overview on novel synthetic approaches and medicinal applications of benzimidazole compounds. *Arabian Journal of Chemistry* **14**, 103418 (2021). <https://doi.org/10.1016/j.arabjc.2021.103418>
11. Pathare, B. & Bansode, T. Review- biological active benzimidazole derivatives. *Results in Chemistry* **3**, 100200 (2021). <https://doi.org/10.1016/j.rechem.2021.100200>
12. Çevik, U. A. *et al.* Synthesis of new benzimidazole derivatives containing 1,3,4 thiadiazole their in vitro antimicrobial in silico molecular docking and molecular. *SAR and QSAR in Environmental Research* **33**, 899-914 (2022). <https://doi.org/10.1080/1062936X.2022.2149620>
13. Dokla, M. E. E. *et al.* SAR investigation and optimization of benzimidazole-based derivatives as antimicrobial agents against Gram-negative bacteria. *European Journal of Medicinal Chemistry* **247**, 115040 (2023). <https://doi.org/10.1016/j.ejmech.2022.115040>
14. Pham, E. C., Vi Thi Leb, T. & Truong, T. N. Design, synthesis, bio-evaluation, and in silico studies of some N-substituted 6-(chloro/nitro)-1H-benzimidazole derivatives as antimicrobial and anticancer agents. *RSC Adv* **12**, 21621 (2022). <https://doi.org/10.1039/D2RA03491C>
15. Hiram, H.-L., Christian J, T.-R. & Socorro, L.-R. A Panoramic Review of Benzimidazole Derivatives and their Potential Biological Activity. *Mini Reviews in Medicinal Chemistry* **22**, 1268-1280 (2022). <https://doi.org/10.2174/138955752266220104150051>
16. Ahamed, F. M. M., Shakya, B. & Shakya, S. Synthesis and characterization of a novel Mannich base benzimidazole derivative to explore interaction with human serum albumin and antimicrobial. *Journal of Biomolecular Structure and Dynamics*, 1-14 (2022). <https://doi.org/10.1080/07391102.2022.2136757>

17. Hussain, S. *et al.* Synthesis of benzimidazole derivatives as potent inhibitors for α -amylase and their molecular docking study in management of type-II diabetes. *Journal of Molecular Structure* **1232**, 130029 (2021). <https://doi.org/10.1016/j.molstruc.2021.130029>

18. Diaconu, D., Antoci, V., Mangalagiu, V., Amariucai-Mantu, D. & Mangalagiu, I. I. Quinoline-imidazole/benzimidazole derivatives as dual-/ multi-targeting hybrids inhibitors with anticancer and antimicrobial activity. *Scientific Reports* **12**, 16988 (2022). <https://doi.org/10.1038/s41598-022-21435-6>

19. Shehab, R. O. & Mansour, M. A. Exploring electronic structure, and substituent effect of some biologically active benzimidazole derivatives: Experimental insights and DFT calculations. *Journal of Molecular Structure* **1223** (2021) **1223**, 128996 (2021). <https://doi.org/10.1016/j.molstruc.2020.128996>

20. Chalkha, M. *et al.* Crystallographic study, biological assessment and POM/Docking studies of pyrazoles-sulfonamide hybrids (PSH): Identification of a combined Antibacterial/Antiviral pharmacophore sites leading to in-silico screening the anti-Covid-19 activity. *J Mol Struct* **1267**, 133605 (2022). <https://doi.org/10.1016/j.molstruc.2022.133605>

21. Bouzaheur, A., Bouchoucha, A., Si Larbi, K. & Zaater, S. Experimental and DFT studies of a novel Schiff base sulfonamide derivative ligand and its palladium (II) and platinum (IV) complexes: antimicrobial activity, cytotoxicity, and molecular docking study. *J Mol Struct* **1261** (2022). <https://doi.org/10.1016/j.molstruc.2022.132811>

22. Dekir, A. *et al.* Novel N-acylsulfonamides: Synthesis, in silico prediction, molecular docking dynamic simulation, antimicrobial and anti-inflammatory activities. *Journal of Biomolecular Structure and Dynamics*, 1-13 (2022). <https://doi.org/10.1080/07391102.2022.2148751>

23. Egbujor, M. C., Okoro, U. C. & Okafor, S. Design, synthesis, molecular docking, antimicrobial, and antioxidant activities of new phenylsulfamoyl carboxylic acids of pharmacological interest. *Med Chem Res* **28**, 2118-2127 (2019). <https://doi.org/10.1007/s00044-019-02440-3>

24. Ghorab, M. M., Soliman, A. M., Alsaid, M. S. & Askar, A. A. Synthesis, antimicrobial activity and docking study of some novel 4-(4,4-dimethyl-2,6-dioxocyclohexylidene)methylamino derivatives carrying biologically active sulfonamide moiety. *Arabian Journal of Chemistry* **13**, 545-556 (2020). <https://doi.org/10.1016/j.arabjc.2017.05.022>

25. Elsisi, D. M. *et al.* Experimental and theoretical investigation for 6-Morpholinosulfonylquinoxalin-2(1H)-one and its hydrazone derivate: Synthesis, characterization, tautomerization and antimicrobial evaluation. *J Mol Struct* **1247** (2022). <https://doi.org/10.1016/j.molstruc.2021.131314>

26. Li, Y. J. *et al.* Human Leukocyte Antigen B*14:01 and B*35:01 Are Associated With Trimethoprim-Sulfamethoxazole Induced Liver Injury. *Hepatology* **73**, 268-281 (2021). <https://doi.org/10.1002/hep.31258>

27. Hampele, I. C. *et al.* Structure and Function of the Dihydropteroate Synthase from *Staphylococcus aureus*. *J. Mol. Biol.* **268**, 21-30 (1997).

28. Dennis, M. L. *et al.* 8-Mercaptoguanine Derivatives as Inhibitors of Dihydropteroate Synthase. *Chemistry* **24**, 1922-1930 (2018). <https://doi.org/10.1002/chem.201704730>

29. Trott, O. & Olson, A. J. AutoDock Vina: improving the speed and accuracy of docking with a new scoring function, efficient optimization, and multithreading. *Journal of computational chemistry* **31**, 455-461 (2010).

30. Shntaif, A. H. *et al.* Rational drug design, synthesis, and biological evaluation of novel N-(2-arylaminophenyl)-2,3-diphenylquinoxaline-6-sulfonamides as potential antimalarial, antifungal, and antibacterial agents. *Digital Chinese Medicine* **4**, 290-304 (2021). <https://doi.org/10.1016/j.dcm.2021.12.004>

31. Arputharaj, D. S., Rajasekaran, M. & Nidhin, P. V. Sulfamethoxazole: Molecular docking and crystal structure prediction. *Results in Chemistry* **5** (2023). <https://doi.org/10.1016/j.rechem.2022.100716>

32. Cheong, M. S. *et al.* Influence of Sulfonamide Contamination Derived from Veterinary Antibiotics on Plant Growth and Development. *Antibiotics (Basel)* **9** (2020). <https://doi.org/10.3390/antibiotics9080456>

33. Roy Chowdhury, D., Ghosh, R., Debnath, S. & Bhaumik, S. Potential peptidyl arginine deiminase type 4 inhibitors from *Morinda citrifolia*: a structure-based drug design approach. *In Silico Pharmacol* **11**, 13 (2023). <https://doi.org/10.1007/s40203-023-00147-3>

34. Ajay, Bemis, G. W. & Murcko, M. A. Designing Libraries with CNS Activity. *Journal of medicinal chemistry* **42**, 4942-4951 (1999). <https://doi.org/10.1021/jm990017w>

35. Zhao, Y. H. *et al.* Evaluation of human intestinal absorption data and subsequent derivation of a quantitative structure-activity relationship (QSAR) with the Abraham descriptors. *J Pharm Sci* **90**, 749-784 (2001). <https://doi.org/10.1002/jps.1031>

36. Bhat, V. & Chatterjee, J. The Use of In Silico Tools for the Toxicity Prediction of Potential Inhibitors of SARS-CoV-2. *Altern Lab Anim* **49**, 22-32 (2021). <https://doi.org/10.1177/02611929211008196>

37. Mitcheson, J. S. hERG Potassium Channels and the Structural Basis of Drug-Induced Arrhythmias. *Chemical research in toxicology* **21**, 1005-1010 (2008). <https://doi.org/10.1021/tx800035b>

38. Finch, A. & Pillans, P. P-glycoprotein and its role in drug-drug interactions. *Australian prescriber* **37**, 137-139 (2014). <https://doi.org/10.18773/austprescr.2014.050>

Figures

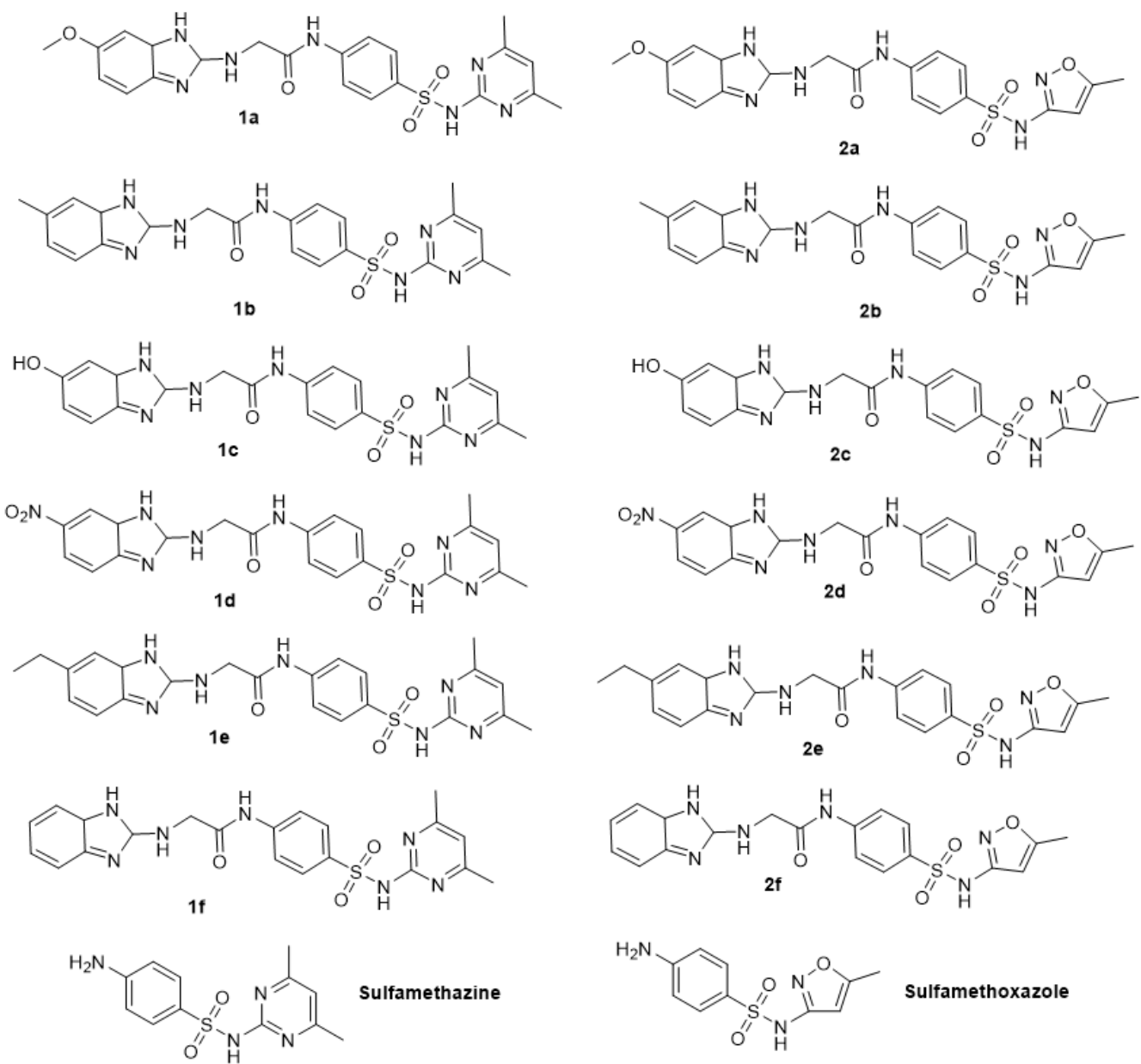
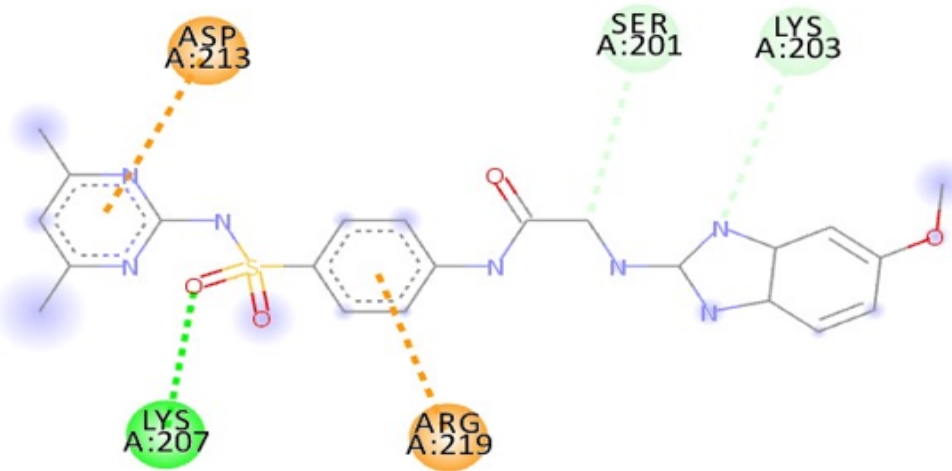


Figure 1

Structure of benzimidazole derivatives



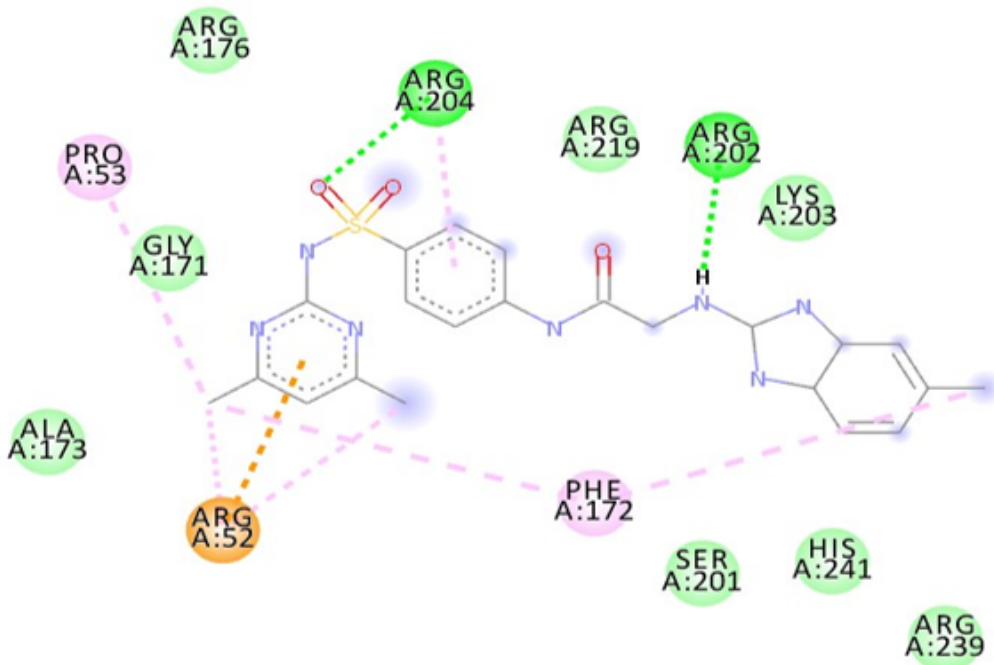
Interactions

Conventional Hydrogen Bond
 Carbon Hydrogen Bond

Pi-Cation
 Pi-Anion

Figure 2

Intermolecular action of 2D interaction between DHPS and Compound **1a**

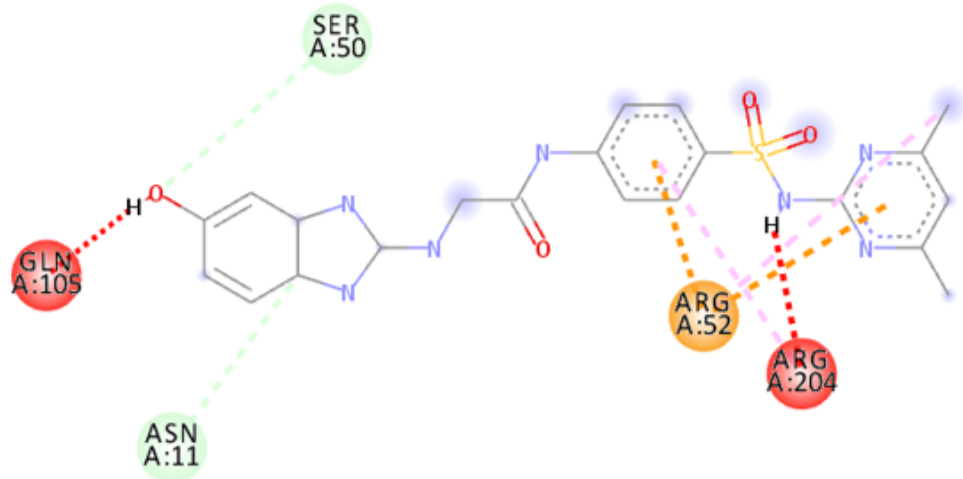


Interactions

van der Waals	Pi-Cation
Conventional Hydrogen Bond	Alkyl
Carbon Hydrogen Bond	Pi-Alkyl

Figure 3

Intermolecular action of 2D interaction between DHPS and compound **1b**



Interactions

Carbon Hydrogen Bond	Alkyl
Unfavorable Donor-Donor	Pi-Alkyl
Pi-Cation	

Figure 4

Intermolecular action of 2D interaction between DHPS and compound **1c**

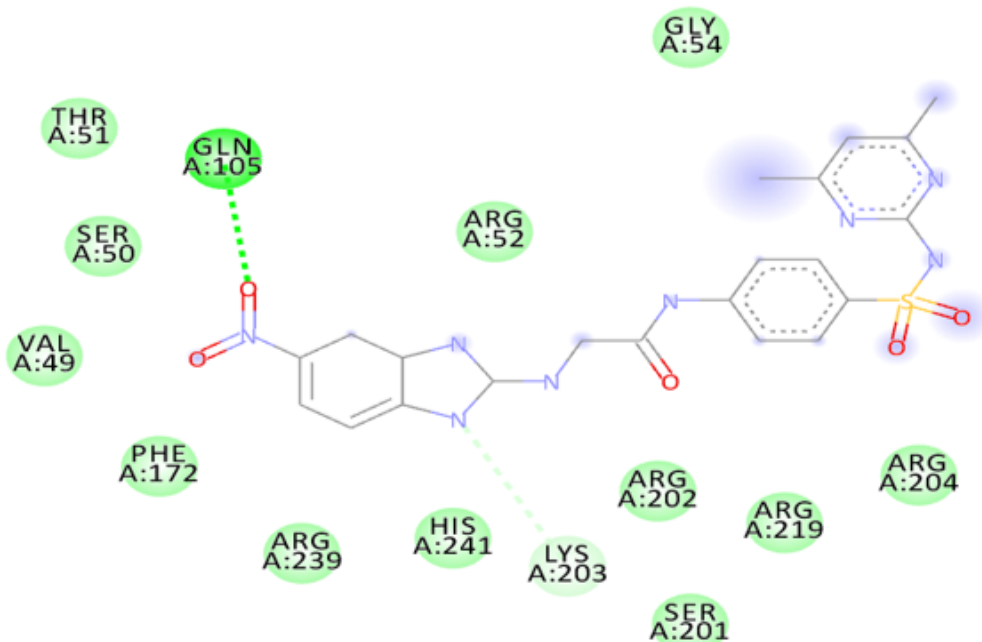
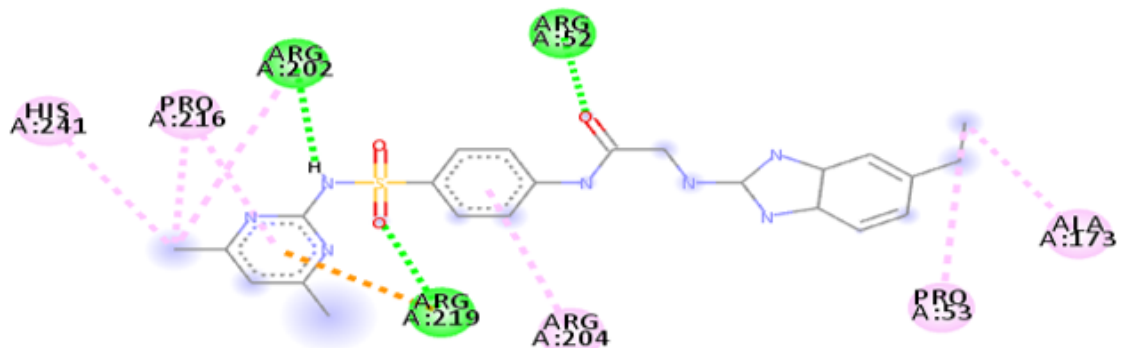


Figure 5

Intermolecular action of 2D interaction between DHPS and compound **1d**



Interactions

Conventional Hydrogen Bond	Alkyl
Carbon Hydrogen Bond	Pi-Alkyl
Pi-Cation	

Figure 6

Intermolecular action of 2D interaction between DHPS and compound **1e**

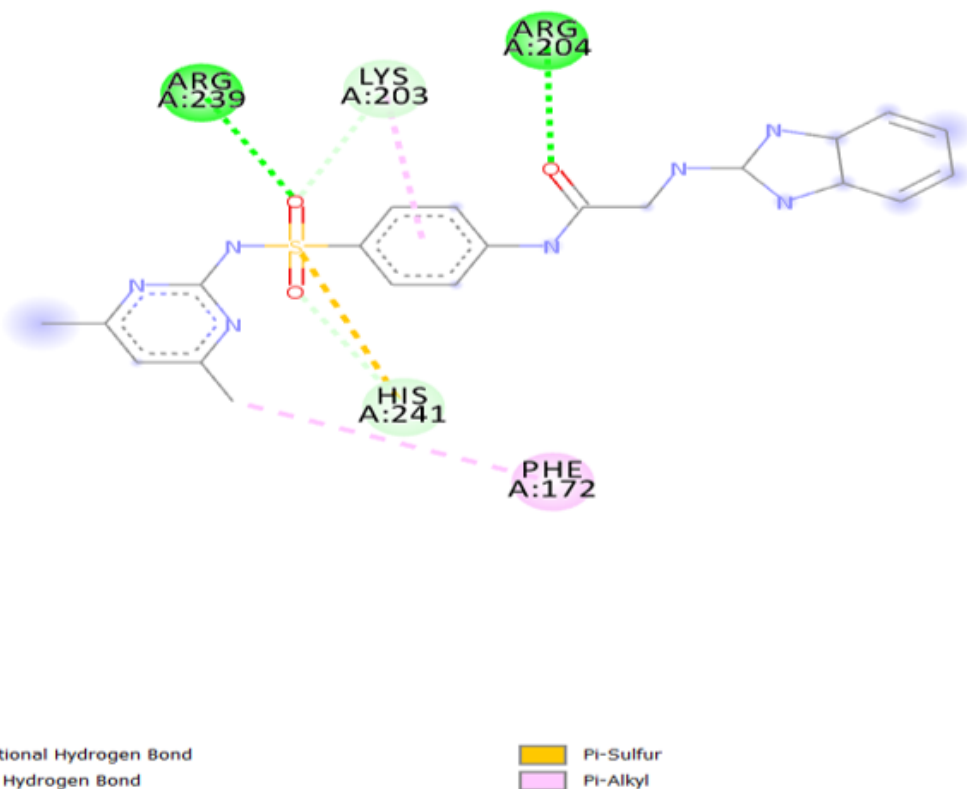
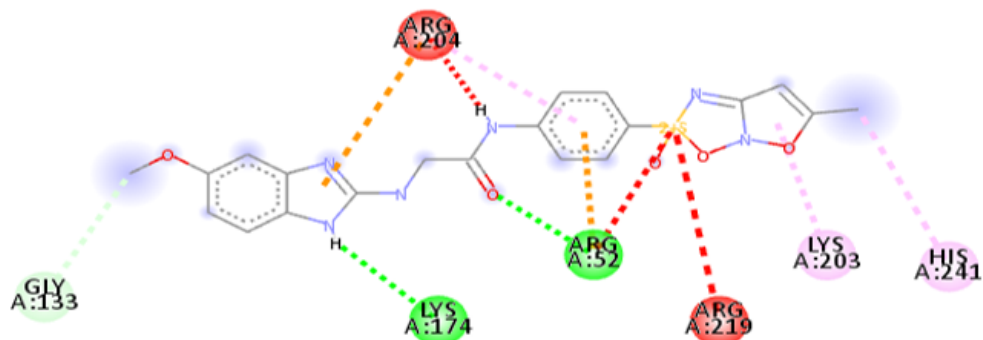


Figure 7

Intermolecular action of 2D interaction between DHPS and compound **1f**



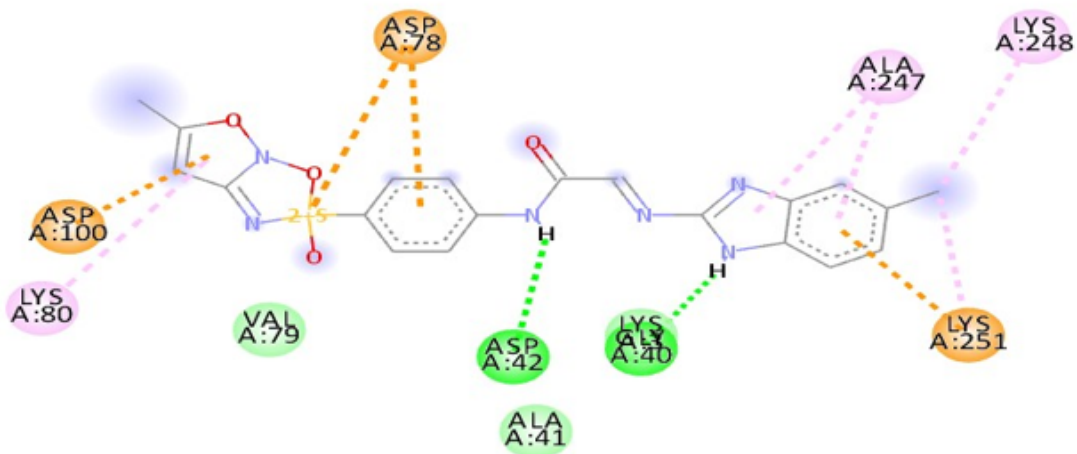
Interactions

- █ Conventional Hydrogen Bond
- █ Carbon Hydrogen Bond
- █ Unfavorable Positive-Positive

- █ Unfavorable Donor-Donor
- █ Pi-Cation
- █ Pi-Alkyl

Figure 8

Intermolecular action of 2D interaction between DHPS and compound **2a**



Interactions

- █ van der Waals
- █ Attractive Charge
- █ Conventional Hydrogen Bond
- █ Pi-Cation

- █ Pi-Anion
- █ Alkyl
- █ Pi-Alkyl

Figure 9

Intermolecular action of 2D interaction between DHPS and compound **2b**

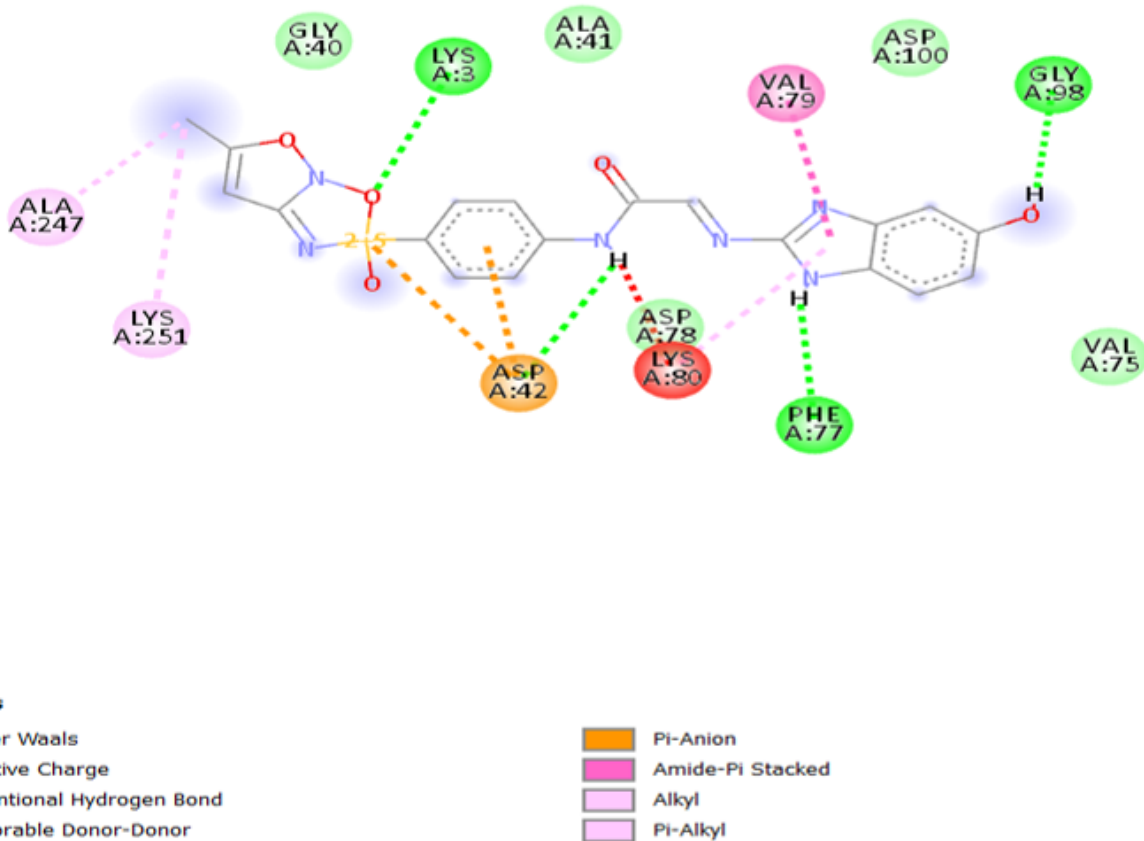


Figure 10

Intermolecular action of 2D interaction between DHPS and compound **2c**

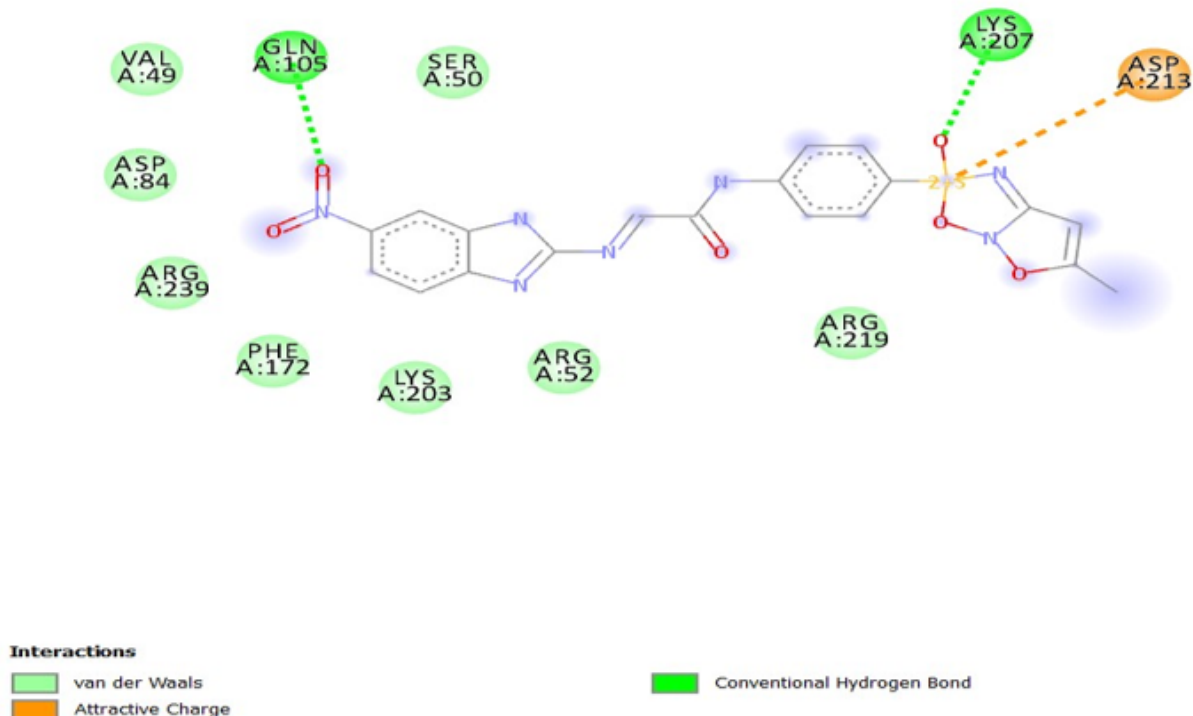


Figure 11

Intermolecular action of 2D interaction between DHPS and compound **2d**

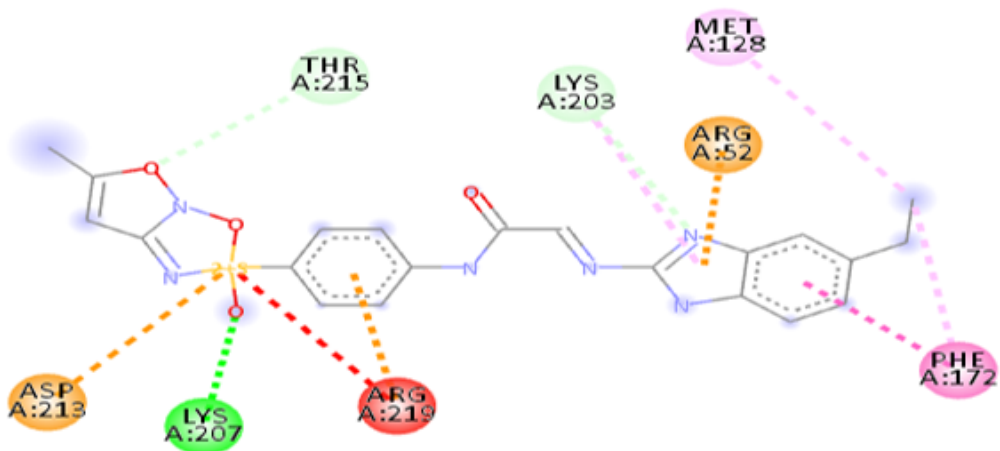


Figure 12

Intermolecular action of 2D interaction between DHPS and compound **2e**

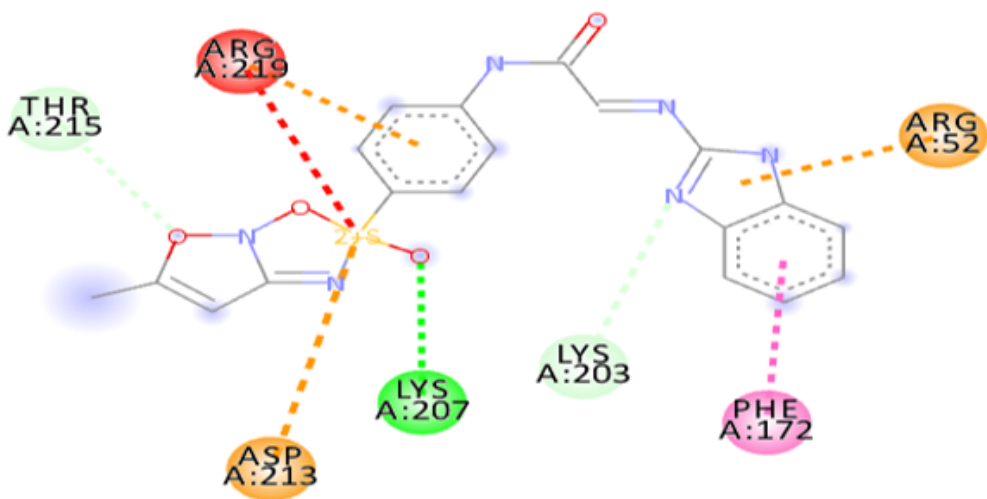


Figure 13

Intermolecular action of 2D interaction between DHPS and compound **2f**

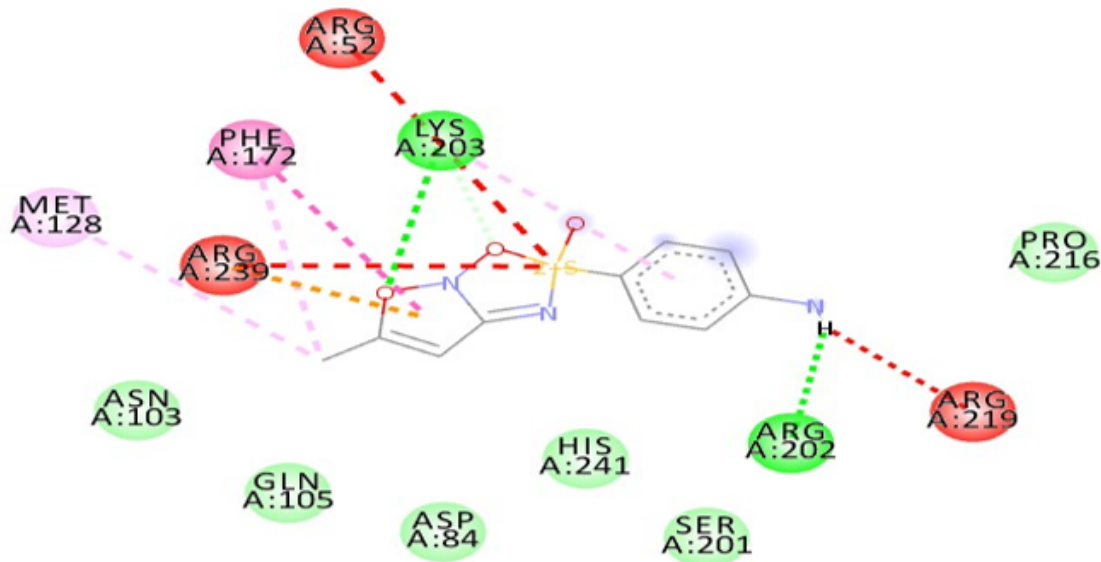
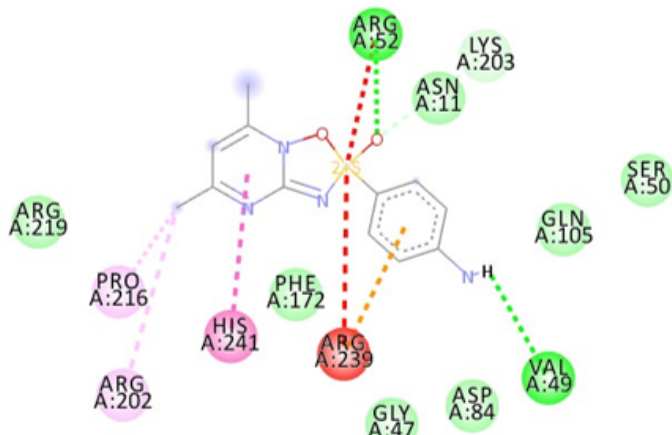


Figure 14

Intermolecular action of 2D interaction between DHPS and sulfamethoxazole.



Interactions

- van der Waals
- Conventional Hydrogen Bond
- Carbon Hydrogen Bond
- Unfavorable Positive-Positive
- Unfavorable Donor-Donor

- Pi-Cation
- Pi-Pi T-shaped
- Alkyl
- Pi-Alkyl

Figure 15

Intermolecular action of 2D interaction between DHPS and **sulfamethazine**.

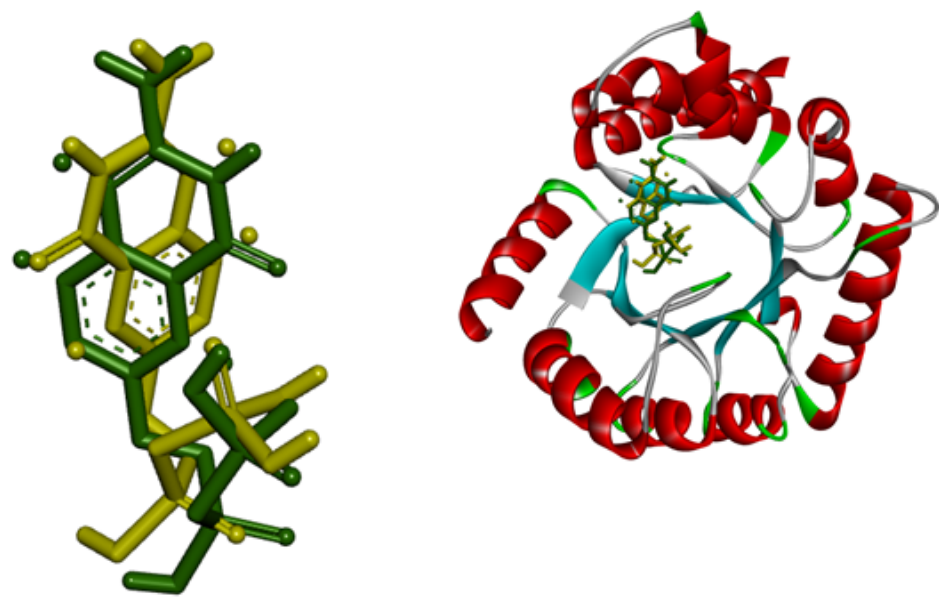


Figure 16

Redocking poses of the co-crystal ligand (PDB ID: 1AD4, natural pose: green, Docked: gold, RMSD: 1.8850)